International Journal of Modern Physics B
Vol. 23, No. 31 (2009) 5819–5834

DOI: 10.1142/S0217979209053436

VIBRATIONAL MODES IN SMALL Ag_n, Au_n CLUSTERS: A FIRST PRINCIPLE CALCULATION

OLCAY ÜZENGI AKTÜRK*,‡, OĞUZ GÜLSEREN† and MEHMET TOMAK*,§

*Department of Physics, Middle East Technical University, 06531 Ankara, Turkey
†Department of Physics, Bilkent University, 06800 Ankara, Turkey
‡uolcay@metu.edu.tr
†gulsere@fen.bilkent.edu.tr
§tomak@ metu.edu.tr

Received 18 September 2008

Although the stable structures and other physical properties of small Ag_n and Au_n, were investigated in the literature, phonon calculations are not done yet. In this work, we present plane-wave pseudopotential calculations based on density-functional formalism. The effect of using the generalized gradient approximation (GGA) and local density approximation (LDA) to determine the geometric and electronic structure and normal mode calculations of Ag_n and Au_n, is studied up to eight atoms. Pure Au_n and Ag_n clusters favor planar configurations. We calculated binding energy per atom. We have also calculated the normal mode calculations and also scanning tunneling microscope (STM) images for small clusters for the first time.

Keywords: First principle calculation; STM image; nanocluster.

PACS numbers: 31.15.E-, 36.40.-c, 61.46.-w, 63.22.Kn

1. Introduction

Metallic clusters have created great interest in recent years because of their surface area to volume ratio and the finite spacing of energy levels with respect to their bulk counterparts.[1] The surface of clusters can completely change their physical properties. Therefore, metallic clusters are technologically important for their catalytic activity and also play a major role in catalysis, colloidal chemistry, and medical science. The main aim of the studies in this field is to investigate the physical features as the size decreases. As a result of decrease in the size, quantum effects become dominant.[2] From the scientific point of view, it is important to understand the atomic structure of clusters starting from interactions between atoms.

The electronic properties and atomic structures of gold and silver clusters have been theoretically investigated by several research groups. Koutecky and coworkers[3,4] investigated small neutral and anionic silver clusters, up to monomer, using Hartree–Fock and correlated *ab initio* method. Fournier studied the silver

clusters using DFT (VWN), sum of square-roots of atomic coordinates, and extended Hückel molecular orbital theory.[5,6] Bravo–Pérez *et al.*[7] investigated small Au_n $n = 26$; clusters by using *ab initio* methods. Lee and co-workers have investigated the structures of pure gold and silver clusters (Au_k and Ag_k, $k = 1$–13) and neutral and anionic gold–silver binary clusters (Au_m Ag_n, $2 \leq k = m + n \leq 7$) by using the density-functional theory with generalized gradient approximation (GGA) and *ab initio* calculations including coupled cluster theory with relativistic *ab initio* pseudo potentials.[2] Wilson and Johnson[8] worked on neutral Au_8 clusters theoretically. It is predicted, using Murrell–Mottram model, that the lowest energy isomer is a D_{2d} dodecahedron, while Hakkinen and Landman[9] used the GGA DFT method with and RECP to predict a T_d copped tetrahedron. Different functionals with LDA/DFT/RECP are used by Wang, Wang and Zhao[10] to determine the stable structure of Au_8 clusters.[11]

Recently, Yoon and co-workers[12] have studied catalytic properties of Au_8 cluster. They have investigated the charging effects on bonding and catalyzed oxidation of CO on Au_8 clusters on MgO. Gold nano clusters on MgO are able to catalyze CO oxidation.[13] Although much of the experimental and theoretical work so far has been done on pure gold and silver clusters and nanoparticles,[2] there exists less information about the normal modes. The only information available is that of experimental data on dimers.[14,15] Therefore, the present work will provide the much needed information on phonons. Before studying physical and electronic properties of Au and Ag clusters, we determine their stable structures.

We thus present in this paper a first principle study of Ag_n and Au_n clusters at neutral states. The structure and energetics of these clusters up to eight atoms are reported. We show that GGA and local density approximation (LDA) are very effective tools to determine the equilibrium. We present interesting results for stable configurations. Electronic properties like density of states (DOS) and scanning tunneling microscope (STM) images are studied. It is possible to determine elasticity by using the normal modes. We calculated the normal modes at the gamma point.

This paper is organized as follows. In Sec. 2, we described computational methods. In Sec. 3, we give our results. Finally, we present the conclusion in Sec. 4.

2. Computational Method

Our calculations are carried out using PWSCF package program[16] based on Density-Functional Theory with a plane-wave basis set. We have used two different approximations: GGA and LDA. We determine the pseudopotential and tested it by comparing with the experimental data. The electron–ion interactions are described by ultrasoft pseudopotentials. We have used the Perdew–Burke–Ernzerhof (PBE) exchange-correlation (xc) and Rabe Rappe Kaxiras Joannopoulos (ultrasoft) potentials for Ag_n clusters,[17] in GGA calculations. For LDA calculations, we have used the Perdew–Zunger (LDA) exchange-correlation (xc) and Rabe *et al.* (ultrasoft) potentials.[18] For Au_n clusters Perdew–Zunger (LDA) xc, and semicore state d

in valence Vanderbilt ultra soft and Perdew–Burke–Ernzerhof (PBE) xc nonlinear core-correction semicore state d in valence Vanderbilt ultrasoft potentials.[17,18]

We tested the cutoff energy. A cutoff energy of 408 eV is used with the plane-wave basis. We carry out our calculations in the super cell because of the lack of periodicity. The binding energy per atom (E_B) is calculated by using

$$E_B = E_{\text{cluster}}/N - E_{\text{atom}}\,, \tag{1}$$

where E_{atom} and E_{cluster} denote the energy of a single atom and the total energy of an atom in the cluster, respectively, and N is the number of atoms in the cluster.

The equilibrium structure is found using Hellmann–Feynman forces. We calculate the STM images using the PWSCF package program[16] based on theory of Tersoff and Hamann.[19] We calculated the normal mode frequency using the Density-Functional Perturbation Theory.[20] Harmonic frequencies and displacement patterns of normal modes on the electronic ground state are calculated from the diagonalization of the dynamical matrix. Vibrational and dielectric properties are calculated using the linear response theory.[21,22] Displacements and frequencies of the normal vibrational modes at the Brillouin zone center are calculated in a harmonic approximation. They are the eigenvectors and square roots of the eigenvalues of the dynamical matrix, respectively. Calculations are performed in a zero macroscopic electric field. Thus, the derived displacements and frequencies are those of the transverse optical modes. In this study, we have calculated the normal modes of Au_n, Ag_n at the Γ point.

3. Results

Firstly, we tested the stability of our results in this work by comparing available experimental data. When the binding energy and bond length are compared the available experimental data for Au_2 in Table 1,[23,24] LDA results are closer to the experimental data than GGA results. We can say that our results are in agrement with experimental data.

The binding energy per atom shows that Au and Ag clusters have planar structures. The stable configurations of Ag and Au clusters are shown in Figs. 1–4 which were drawn by XCrySDEN (Crystalline Structures and Densities) program.[25] The cited works in the literature show that, generally, Au clusters have planar structures (2D), while Ag clusters have both 2D and 3D structures. As seen in Fig. 1, Au clusters favor planar structures with GGA. Au_3 shows a triangular structure. Au_4 favors a parallelepiped. But, Au_5, Au_6, and Au_7 show two stable structures.

Table 1. The dimer length and binding energy of Au clusters.

Au_2	GGA	LDA	Experimental
Dimer (Å)	2.523	2.432	2.470
Binding energy (eV)	2.244	2.954	2.290 ± 0.008

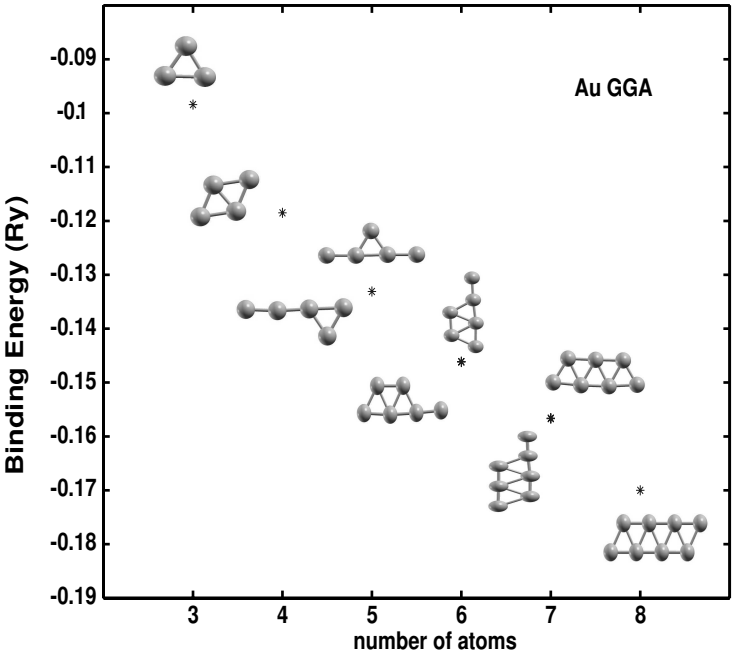

Fig. 1. GGA results for stable configuration of Au clusters.

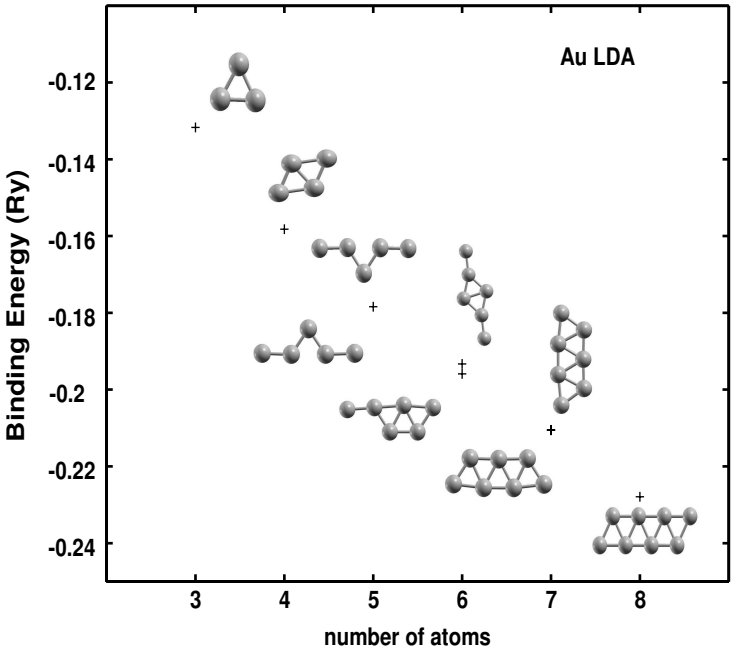

Fig. 2. LDA results for stable configuration of Au clusters.

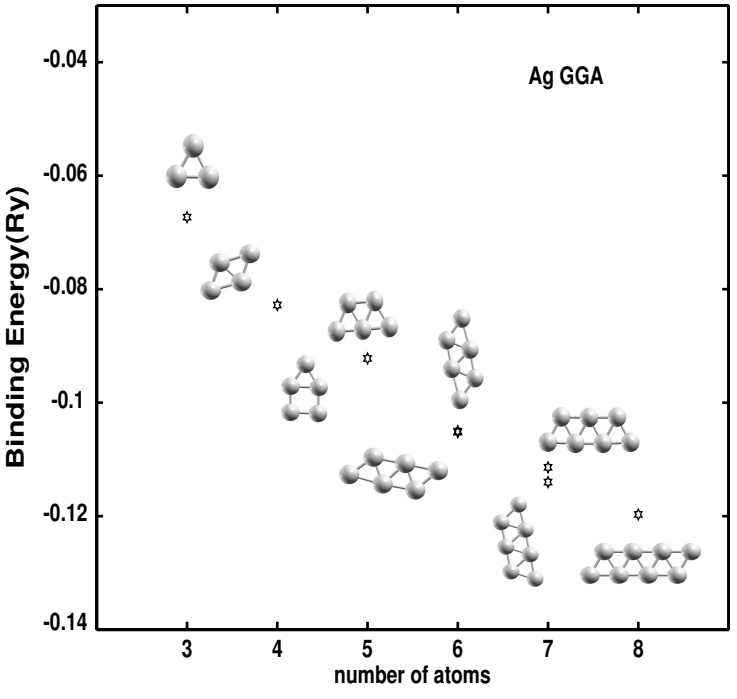

Fig. 3. GGA results for stable configuration of Ag clusters.

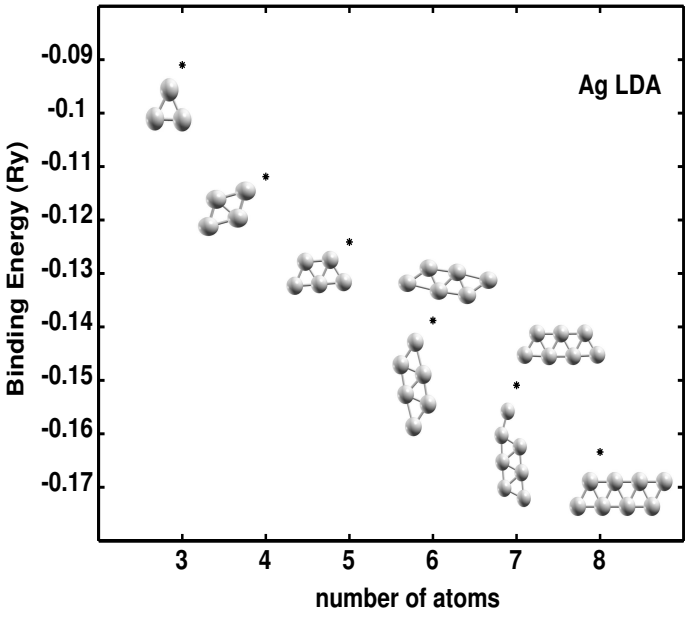

Fig. 4. LDA results for stable configuration of Ag clusters.

Table 2. The dimer length and binding energy of Ag clusters.

Ag_2	GGA	LDA	Experimental
Dimer (Å)	2.589	2.174	2.53
Binding energy (eV)	0.850	1.070	0.83

Some structures are not symmetrical. Although, we tried to test the stable configurations already reported in the literature,[2,8–10,13,26] the stable structures we found turned out to be different. These difference comes from using different methods. These differences are also due to binding energy. We found that the binding energy of configuration in the literature are smaller than our stable configurations for Au and Ag clusters. Because of that reasons, our structures are more stable than the structures of literature. Although, the stable configuration of Au_5 is in agreement with G. Bravo–Pérez *et al.*'s results,[7] we obtain the different frequency from it. We also obtain the stable configuration of Au_8. Au_8 and Au_4 have similar shapes.

As seen in Fig. 2, Au clusters show planar structures with LDA. The same shapes are found as with GGA up to four atoms. Au_5, Au_6, and Au_7 show two stable structures like in GGA. But, Au_5 and Au_6 have different shapes than in GGA. Some structures are not symmetrical like in GGA. Au_7 and Au_8, show the same structures as in the GGA.

As seen in Table 2, our results are in general agreement with the experimental data.[15,27] Figure 3 shows that Ag_3 has triangular structure although we begin with an initial open angle configuration. For Ag_4, a parallelepiped is the most stable configuration. Ag_5 has two stable configurations. In addition to the shape of Ag_4, there exists another configuration which is different from that in the literature.[2–6,28] Ag_6 and Ag_7 show similar structures to Ag_5. Ag_8 is like Ag_4 but different from that in the literature.[2–6] They found that Ag clusters undergo a 2D to 3D geometry transition from Ag_6 to Ag_7. We do not observe this transition. This may come from using different pseudopotential and wave function basis set. The shapes of the Ag_7 and Ag_8 are similar to Au_7 and Au_8, respectively.

The GGA structures for Ag_3, Ag_4, Ag_6, Ag_7, and Ag_8 are similar to that with LDA as shown in Fig. 4. But for Ag_5, we find only one stable structure.

We have calculated DOS and partial density of states (PDOS) of the stable structure of Au for GGA and LDA. GGA result is in agrement with LDA. As an example, Au_8 for LDA is given in Fig. 5. Figure 5 shows that *sp* orbital overlap orbital near the Fermi surface in the highest occupied molecular orbital(HOMO) and lowest unoccupied molecular orbital (LUMO), This shows that there is *s*–*p* hybridization. The effects of *d*-orbitals are weak. It can be said that *s*–*d* hybridization in the LUMO is weaker than that in the HOMO. It is known that the major contribution to the weak *s*–*d* hybridization in the nonrelativistic calculations, comes from the *s* orbital.[29]

We have calculated the DOS and PDOS of Ag clusters for GGA and LDA. As an example, Ag_8 is given in Fig. 6 for LDA. GGA PDOS and DOS are similar to

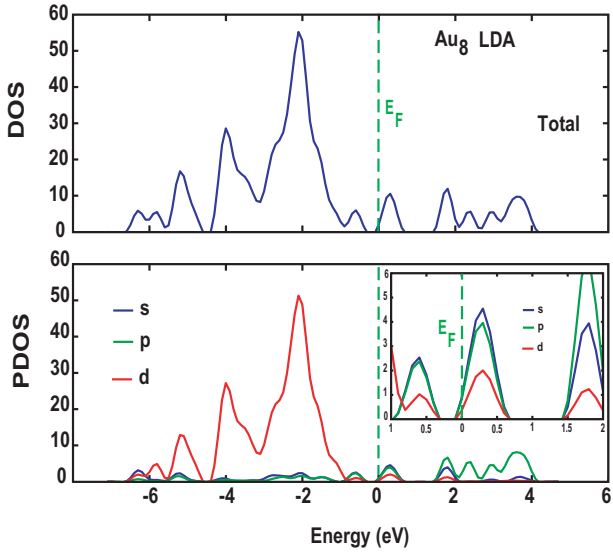

Fig. 5. DOS and partial DOS of Au_8 LDA.

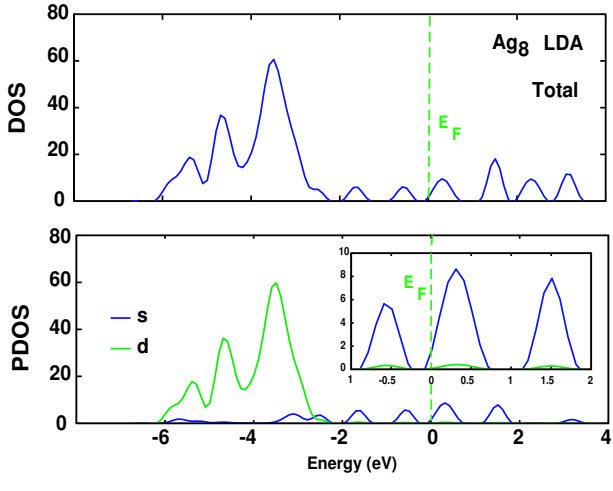

Fig. 6. DOS and partial DOS of Ag_8 LDA.

that in LDA. The major contribution comes from the *s* orbital in both HOMO and LUMO. While *s*–*d* hybridization in the HOMO is strong, it is weak in the LUMO.

Here, we present for the first time, the STM images for small clusters investigated in this work. STM images are important for investigation of adsorption of molecules on surfaces. Bonding properties and hybridization can be clearly seen in STM images. We calculated the STM images at constant current and positive and

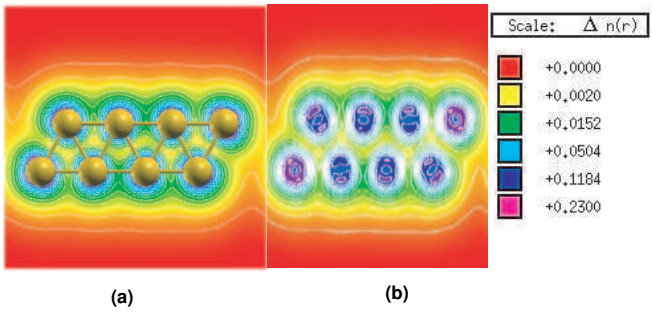

Fig. 7. STM image for HOMO of Au_8 GGA.

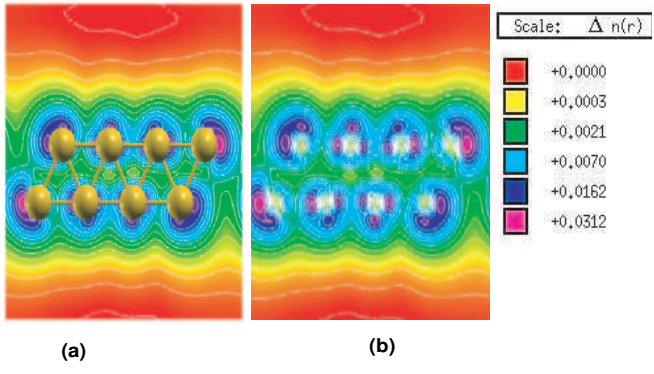

Fig. 8. STM image for LUMO of Au_8 GGA.

negative bias voltage of 2.45 and −2.45 eV, respectively for Au_8 and Ag_8 in GGA and LDA.

STM images of Au_8 with LDA results are in agreement with GGA. As an example, STM image of Au_8 for HOMO GGA is given in Figs. 7(a) and 7(b). As seen in the figure, the charge density between atoms is bigger, which results in covalent bonds. Figure 7(b) shows the density in more detail. s–p hybridization is seen in the leftmost bottom atom and the rightmost top atom and also in the atoms at the middle. The strongest binding is in the rightmost bottom and the leftmost top atoms as seen in the charge distribution. Figure 8(a) and 8(b) show that s–p^2 hybridization occurs between the atoms at the middle in the LUMO. s–p hybridization is seen also in the top and bottom atoms, where the binding is stronger.

We have calculated STM images of Ag_8 for GGA and LDA. LDA results are in agreement with GGA. As an example, STM images of Ag_8 in GGA are given in Figs. 9, 10(a) and 10(b), charge distribution between atoms is denser, as in Au_8. In the HOMO and LUMO, the s orbital is more effective than d orbital. Binding in the top and bottom atoms is stronger.

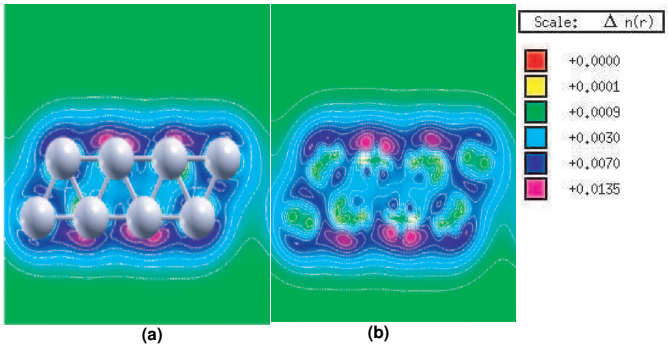

Fig. 9. STM image for HOMO of Ag_8 GGA.

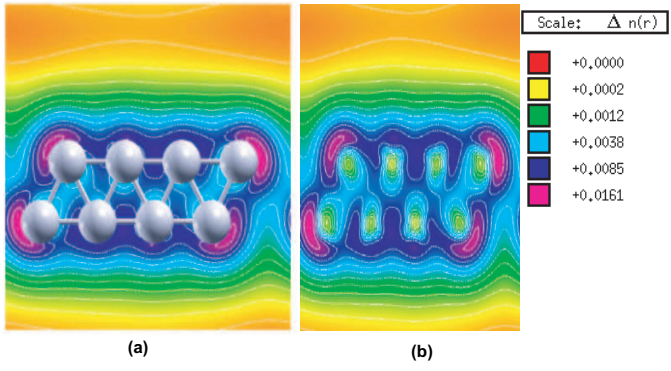

Fig. 10. STM image for LUMO of Ag_8 GGA.

Table 3. The normal mode frequency of Au_2 and Ag_2.

	GGA	LDA	Experimental
Au_2 ω (cm^{-1})	172.99	204.92	191.00
Ag_2 ω (cm^{-1})	138.65	202.49	192.4

We have also calculated modes of vibrations of Au and Ag for GGA and LDA and these are given Figs. 11–14. We give only the three highest frequencies. Thus, we tested the stable structures which we found.

We compare the normal modes of Au_2 and Ag_2 with available experimental data in Table 3.[14,15] The normal mode frequencies of Au_2 and Ag_2 with the LDA is closer to the experimental data than with the GGA result. We see that our results are in agreement with the experimental data. We have calculated the normal modes of Ag and Au. As an example, we show only the vibration modes of the three highest frequencies in Figs. 11–14 for Ag and Au.

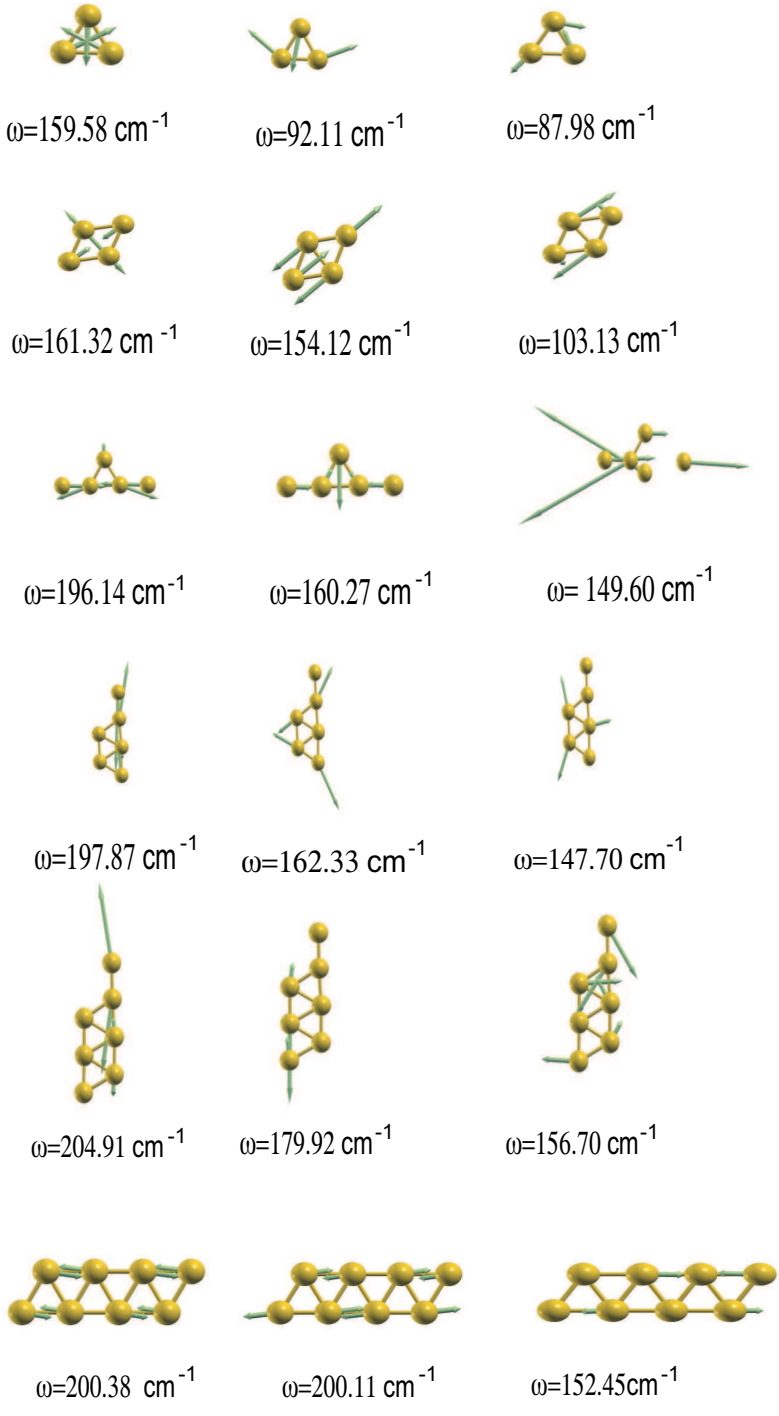

Fig. 11. Vibration modes of stable configuration of Au_n clusters obtained by using GGA.

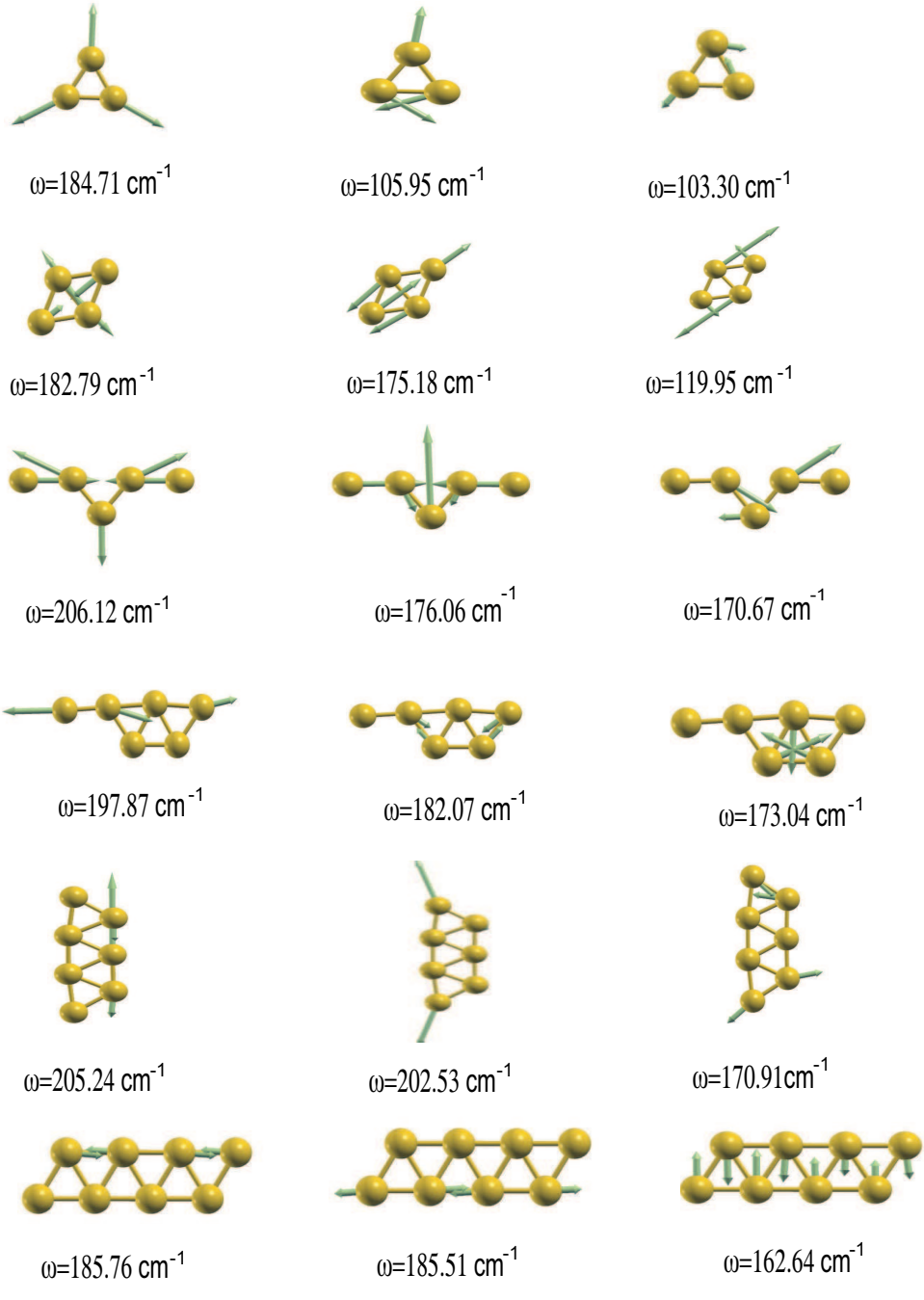

Fig. 12. Vibration modes of stable configuration of Au_n clusters obtained by using LDA.

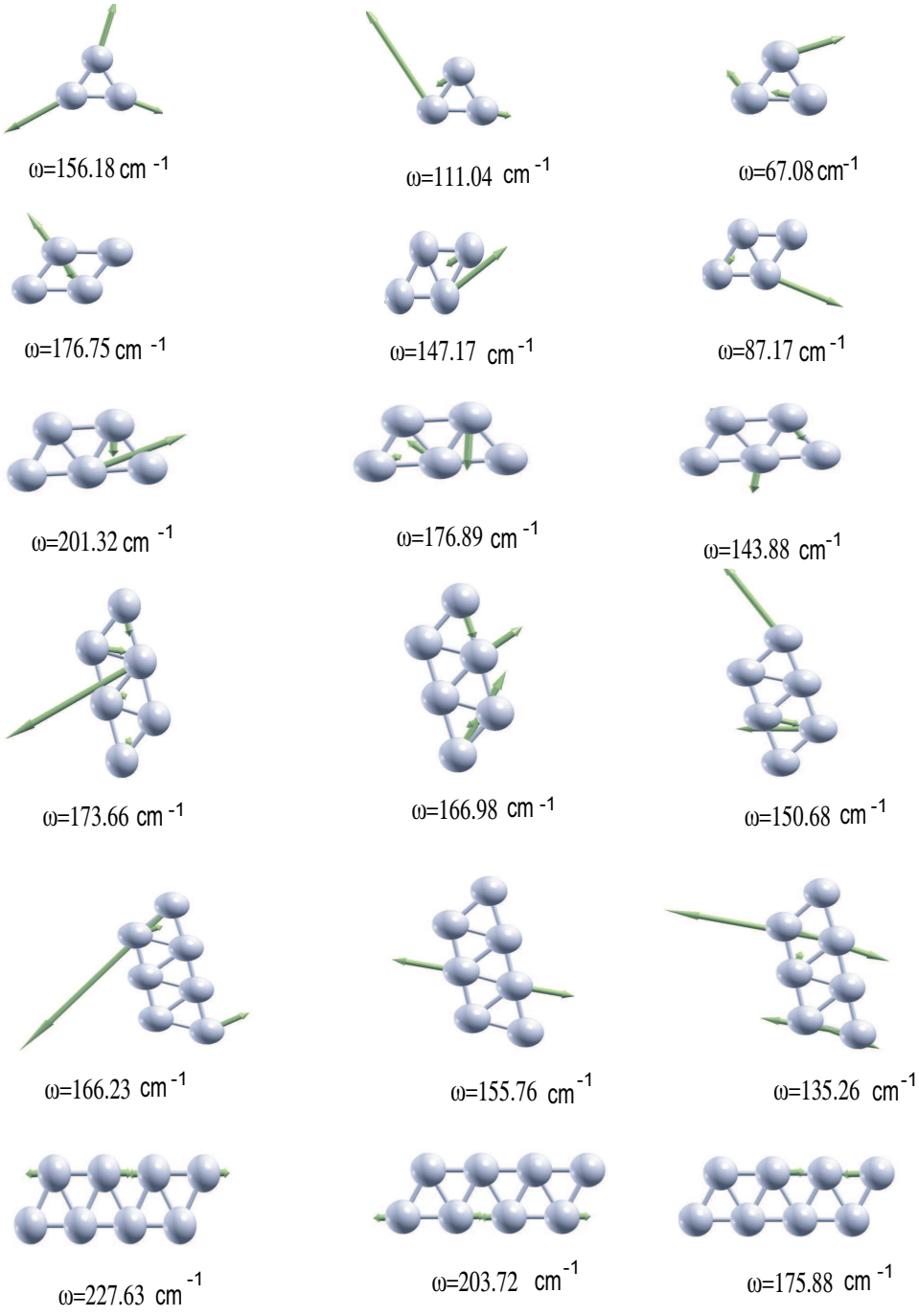

Fig. 13. Vibration modes of stable configuration of Ag_n clusters within GGA.

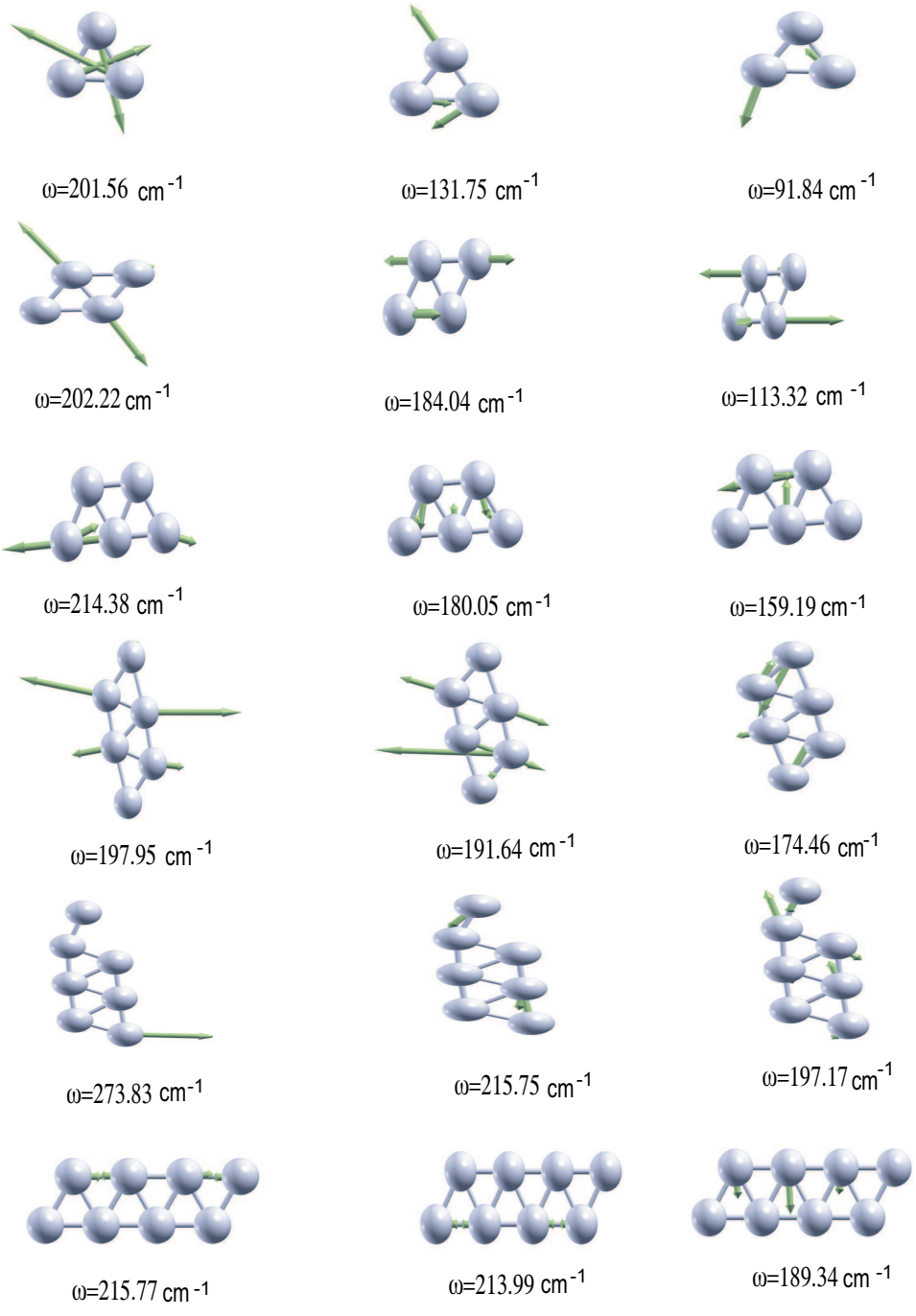

Fig. 14. Vibration modes of stable configuration of Ag_n clusters within LDA.

As seen in Fig. 11, for GGA, $\omega = 159.58$ cm^{-1} shows the symmetric stretching in Au_3, the other two frequencies correspond to the antisymmetric stretching. In Au_4, all frequencies correspond to antisymmetric stretching modes. In Au_5, $\omega = 196.14$ cm^{-1} shows the combination of scissor and antisymmetric stretching. This frequency is smaller than frequency in the literature.[7] Other frequencies correspond to antisymmetric stretching. In Au_6, $\omega = 147.70$ cm^{-1} is for the symmetric stretching, others correspond to the antisymmetric stretching. In Au_7, $\omega = 179.92$ cm^{-1} is for scissor stretching, all of the other frequencies correspond to antisymmetric stretching. In Au_8, $\omega = 200.38$ cm^{-1} and $\omega = 200.11$ cm^{-1} correspond to the scissor stretching.

As seen in Fig. 12, all frequencies for Au_4 correspond to the similar modes in both LDA and GGA. While $\omega = 185.76$ cm^{-1}, $\omega = 185.51$ cm^{-1} in the Au_8, $\omega = 182.07$ cm^{-1} in the Au_6 correspond to the scissor stretching, $\omega = 185.51$ cm^{-1} in the Au_8 is for the combination of scissor and symmetric stretching. As $\omega = 184.71$ cm^{-1} in Au_3 and $\omega = 173.04$ cm^{-1} in Au_6 are for the symmetric stretching, others correspond to the antisymmetric stretching.

Fournier[5,6] calculated the normal mode of some stable configurations of Ag clusters. Fournier found that there is a noticeable jump in the largest frequency from $N = 6$ to $N = 7$ clearly due to the change from planar to 3D structure. We do not observe this transition.

The vibration normal modes of Ag are given in Fig. 13 for GGA, while $\omega = 155.76$ cm^{-1} in the Ag_7 correspond to the scissor stretching, $\omega = 227.63$ cm^{-1} and $\omega = 203.72$ cm^{-1} in Ag_8 are for the combination of symmetric stretching and scissor stretching. While $\omega = 156.58$ cm^{-1} in the Ag_3 correspond to the symmetric stretching, the others correspond to the antisymmetric stretching.

The vibration normal modes of Ag are given in Fig. 14 for LDA, $\omega = 202.22$ cm^{-1} in the Ag_4, $\omega = 197.95$ cm^{-1} in the Ag_6, $\omega = 215.77$ cm^{-1} and $\omega = 213.99$ cm^{-1} in the Ag_8 are for the scissor, $\omega = 273.83$ cm^{-1} in the Ag_7 correspond to the the stretching. While $\omega = 189.34$ cm^{-1} in the Ag_8 is for the symmetric stretching, the others correspond to the antisymmetric stretching. As a result, the same structure of Au and Ag clusters have different vibrational frequencies, as seen in Au_8 and Ag_8, because of having different mass. It is well-known that mass of Au atom are bigger than Ag. According to normal mode calculation methods, the frequency and mass are inversely related. Therefore, the vibration frequencies of Ag clusters are greater than Au clusters for same structure. On the other hand, the same vibrational modes within Ag_4 and Ag_3 are smaller than the same structure of Au clusters due to having different angle and bonding properties.

4. Conclusion

In this report, Au and Ag clusters are studied by using DFT. We have used GGA and LDA approximations. The electron–ion interaction is described by the ultrasoft pseudopotentials. We determined the stable structures of these clusters and

compared with the available experimental data. Our results are in agreement with experimental data for dimer.We find that both Ag and Au clusters have planar structures.

STM images and DOS are calculated for Ag_8 and Au_8. For Au cluster, We see that there exists a hybridization in both DOS and STM and that covalent binding is more effective. For Ag clusters, *s* and *d* orbitals are involved in metallic binding which is more effective than covalent binding. We present for the first time normal mode of Ag and Au clusters, only available information is normal mode of dimer, and should be helpful to understanding the elastical properties of clusters.

Acknowledgments

This work was supported by METU Graduate School of Natural and Applied Sciences (No: BAP-2006-07.02-00-01).

References

1. L. Xiao and L. Wang, *J. Phys. Chem. A* **108**, 8605 (2004).
2. H. M. Lee, M. Ge, B. R. Sahu, P. Tarakeshwar and K. S. Kim, *J. Phys. Chem. B* **107**, 9994 (2003).
3. V. B. Koutecky, L. Cespiva, P. Fantucci and J. Koutecky, *J. Chem. Phys.* **98**, 7981 (1993).
4. V. B. Koutecky, L. Cespiva, P. Fantucci, J. Pitner and J. Koutecky, *J. Chem. Phys.* **100**, 490 (1994).
5. R. Fournier, *J. Chem. Phys.* **115**, 2165 (2001).
6. K. A. Bosnick, T. L. Haslett, S. Fedrigo, M. Moskovits, W.-T. Chan and R. Fournier, *J. Chem. Phys.* **111**, 8867 (1999).
7. G. Bravo-Pérez, I. L. Garzón and O. Novaro, *J. Mol. Struct.: (Theochem)* **493**, 225 (1999).
8. N. T. Wilson and R. L. Johnston, *Eur. Phys. J. D* **12**, 161 (2000).
9. H. Häkkinen and U. Landman, *Phys. Rev. B* **62**, R2287 (2000).
10. J. Wang, G. Wang and J. Zhao, *Phys. Rev. B* **66**, 35418 (2002).
11. R. M. Olson, S. Varganov *et al.*, *J. Am. Chem. Soc.* **127**, 1049 (2005).
12. B. Yoon *et al.*, *Science* **307**, 403 (2005).
13. A. V. Walker, *J. Chem. Phys.* **122**, 094310 (2005).
14. D. Sánchez-Portal, E. Artacho, J. Junquera, P. Ordejn, A. Garcia and J. M. Soler, *Phys. Rev. Lett.* **83**, 19 (1999).
15. J. R. Lombardi and B. Davis, *Chem. Rev.* **102**, 2431 (2002).
16. S. Baroni, A. Dal Corso, S. de Gironcoli and P. Giannozzi, ⟨http://www.pwscf.org⟩.
17. J. P. Perdew, K. Burke and M. Ernzerhof, *Phys. Rev. Lett.* **77**, 3865 (1996).
18. J. P. Perdew and A. Zunger, *Phys. Rev. B* **23**, 5048 (1981).
19. J. Tersoff and D. R. Hamann, *Phys. Rev. B* **31**, 2 (1985).
20. A. D. Corso, A. Pasquarello and A. Baldereschi, *Phys. Rev. B* **56**, R11369 (1997).
21. S. Baroni, P. Giannozzi and A. Testa, *Phys. Rev. Lett.* **58**, 1861 (1987).
22. P. Giannozzi, S. de Gironcoli, P. Pavone and S. Baroni, *Phys. Rev. B* **43**, 7231 (1991).
23. B. H. Billings and D. E. Gray, *American Institute of Physics Handbook*, 3rd edn. (McGraw-Hill, New York, 1972).
24. B. Simard and P. Hackett, *J. Mol. Spec.* **142**, 310 (1990).

25. A. Kokalj, *Comp. Mat. Sci.* **28**, 155 (2003). ⟨www.xcrysden.org⟩.
26. J. Oviedo and R. E. Palmer, *J. Chem. Phys.* **117**, 9548 (2002).
27. K. Hilpert and K. A. Gingerich, *Ber. Bunsenges. Phys. Chem.* **84**, 739 (1980).
28. E. M. Fernández, J. M. Soler, I. L. Garzón and L. C. Balbás, *Phys. Rev. B* **70**, 165403 (2004).
29. X. Gu, M. Ji, S. H. Wei and X. G. Gong, *Phys. Rev. B* **70**, 205401 (2004).